RSC Advances

ROYAL SOCIETY OF CHEMISTRY

www.rsc.org/advances

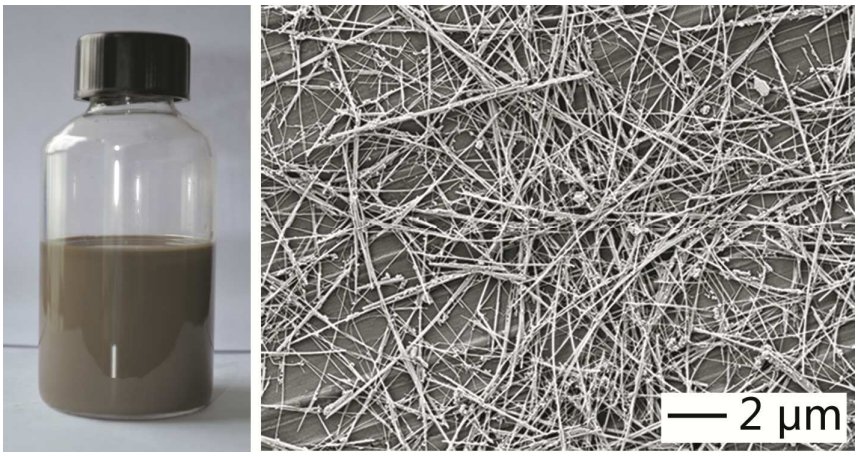

Silver nanowires capped with oleyamine molecules has been prepared in high p urity for the first time.

Revised Manuscript RA-ART-07-2015-013884

Facile Synthesis of Oleyamine-Capped Silver Nanowire and Its Application for Transparent Conductive Electrode**

Jun Zhu,[a] Xiufang Xu,[b] Jinglei Liu,[c] Yiqun Zheng,[b] and Shifeng Hou[a, c]*

[a]Research Institute of Bio-nanotechnology, Jining Medical University, Jining, Shandong 272000, P. R. China

[b]Leadernano Tech L.L.C., Jining, Shandong 272000, P. R. China

[c]National Engineering and Technology Research Center for Colloidal Materials, Shandong University, Jinan, Shandong 250100, P. R. China

*Corresponding Author: Prof. J. Zhu, E-mail: jnzhuj@163.com

Abstract

We report a facile method for the synthesis of oleyamine-capped silver (Ag) nanowires in high purity. For the first time, Ag nanowires could be produced in high purity via a simple one-pot approach in hydrophobic phase. The success of this synthesis relies on the use of Cu^{2+} to mediate the reduction of silver bromide (AgBr) by oleyamine at an elevated temperature, which promoted the high-yield formation of Ag products with a wire-like shape. These Ag nanowires were washed and deposited on PET films to form transparent conductive electrode (TCE), which showed a sheet resistance of 34.0 Ω/sq and an optical transmittance of 70-80% at visible wavelength. In addition to TCE, these nanowires could also find important applications in the fields of conductive ink, wearable electronics, among others.

Keywords: silver nanowires; nanocrystals; oleyamine; hydrophobic; transparent conductive electrode.

INTRODUCTION

One-dimensional metallic nanocrystals have attracted significant research attentions in the past decades due to their unique electronic, optical, thermal, and catalytic properties.[1-13] Among these metals, silver (Ag) nanowire has been an area of active research because Ag exhibits the highest electrical and thermal conductivities.[14-21] Owing to these merits, Ag has made its nanowires attractive building blocks for the application in photonic, electronic, and sensing fields. For example, Ag nanowires have been considered as one of the most promising candidate to replace tin-doped indium oxide (ITO) to serve as the transparent conductive electrode (TCE) for the next-generation display device with flexible characteristic.[22-27]

Thanks to research efforts contributed by many groups, several synthetic approaches have been proposed and validated for the fabrication of metallic nanowires with reasonable yields (e.g., template assisted in-plane growth of nanowires, electric field assisted growth of nanowires, among others).[28-31] Compared to physical routes, wet-chemical synthesis exhibited tremendous advantages, such as template-free, low cost, easy to scale up, mild reaction condition, among others.[32-39] Take silver for example. As a pioneer in this field, Xia and coworkers demonstrated that high-quality Ag nanowires could be obtained in a way that ethylene glycol solutions of $AgNO_3$ and poly(vinylpyrrolidone) (PVP) were dropwisely added at an elevated temperature.[40-43] This method was further improved and optimized to overcome several drawbacks, such as long reaction times, low wire-to-particle yields, irregular wire morphologies, and low aspect ratios.[44, 45] In addition to the use of ethylene glycol as the solvent, other reagents were also employed.[46-48] For example, Murphy and coworkers reported the synthesis of make crystalline silver nanowires in water, in the absence of a surfactant or polymer to direct nanoparticle growth. Wong and coworkers reported a facile preparation method for Ag nanowires with uniform diameters of 60±2 nm where glycerol was used as the solvent.[48] All these reports have contributed to the development of synthetic protocols for Ag nanowires fabrications.

Despite these successful demonstrations, it is worth noting that there has been no report about synthesis of Ag nanowires in hydrophobic phase yet. When the Ag nanowires were capped with hydrophilic molecules, it is difficult to mix and suspend them with hydrophobic materials (e.g., oil, resin, among others) homogeneously, which limits their further applications. To this end, it is highly desirable to develop a convenient approach for production of Ag nanowires capped with hydrophobic molecules and extended their use for more applications in hydrophobic systems.

The use of metallic cations to mediate the shape-controlled synthesis of noble metals has ar oused enormous research attentions recently.[49-51] Typically, the addition of a secondary metal precursor with trace amount in the synthesis can react with the major metal through specific adsorption or coordination significantly, thus change the growth pattern of the major metal. Take copper cations for example. Xia and coworkers reported the use of Cu^{2+} to reduce the amount of free Ag^{+} during the formation of initial seeds and scavenge adsorbed oxygen from the surface of the seeds once formed in the synthesis of Ag nanowires.[45] Xie and coworkers synthesized Au-Pd alloyed nanocrystals with a special hexoctahedral (HOH) shape via a Cu^{2+}-mediated reaction.[52] For these demonstrations, the role of copper cations are considered to influence the reaction kinetics and/or varying the crystal plane growth via underpotential deposition.

Herein, we describe a facile route to the fabrication of high-purity Ag nanowires capped with hydrophobic molecules, oleyamine (OAm). The success of this synthesis relies on the use of copper chloride ($CuCl_2$) to mediate the reduction of silver bromide (AgBr) by OAm at an elevated temperature. To the best of our knowledge, it is the first time that hydrophobic molecules-capped Ag nanowires could be produced in high purity via a simple one-pot method. To understand the formation mechanism, we monitored the process by terminating the reaction at different stages and taking out the aliquot for SEM imaging. In addition, the amount of $CuCl_2$, reaction temperature, and type of Ag precursor were also evaluated to reveal their impacts on the final product morphology. These oleyamine-capped Ag nanowires were then washed and

deposited on PET films to form TCE, which showed a sheet resistance of 34.0 Ω/sq and an optical transmittance of 70-80% at visible wavelength. This work provides a feasible strategy to synthesize one-dimensional Ag nanomaterials in hydrophobic phase, which can be potentially extended to other noble metals.

Experimental

Materials. Silver bromide (AgBr, ≥99.0%), anhydrous copper chloride ($CuCl_2$, 99.99%), oleyamine (OAm, 80-90%), and hexane were all obtained from Aladdin Industrial Inc. and used as received. Silver chloride (AgCl, ≥99.5%) and silver nitrate ($AgNO_3$, ≥99.8%) were obtained from Sinopharm Chemical Reagent Co., Ltd. and used as received. $CuCl_2$-OAm solution (0.3 g/L) was prepared by mixing 3 mg of $CuCl_2$ in 10 mL of OAm at 60 ^oC for 10 min and cooled down to room temperature naturally.

Synthesis of OAm-capped Ag nanowires. For a typical synthesis, 600 mg of AgBr, 0.1 mL of $CuCl_2$-OAm solution (0.3 g/L), and 30 mL of oleyamine were added to a 250 mL round bottle flask to which a stir bar was added. The concentration of Ag ions in the reaction system was 106.5 mM. The flask was then suspended and heated using a heating mantle under magnetic stirring (300 rpm). The reaction was allowed to continue for 6 hours and then quenched by cooling the flask in a room-temperature water bath. Products were then centrifuged at 6000 rpm for 10 minutes, washed with hexane three times, and stored in hexane for further use and characterization.

Preparation of TCE films composed of Ag nanowires. For a typical process, the as-prepared hexane solution containing Ag nanowires was directly applied onto a piece of PET film. Meyer rod was used to make sure the film with homogeneously coated with the solution. Then the films were dried in air at room temperature for further use and characterization.

Instrumentation. Scanning electron microscopy (SEM) images were captured using an Ultra Plus microscope operated at 3.0 kV (Zeiss, Oberkochen, Germany). The samples were prepared

by dropping suspensions of nanowires onto Cu foils. High-resolution TEM (HRTEM) images and electron diffraction patterns were obtained using a field-emission JEM-2100F microscope operated at 200 kV (JEOL, Tokyo, Japan). The samples were prepared by dropping suspensions of nanowires onto carbon-coated Cu grids and dried under ambient conditions. X-ray diffraction (XRD) patterns were recorded by using a diffractometer with filtered Cu K_α radiation at 0.154 nm. All extinction spectra were recorded using a Persee TU-1900 UV-vis-NIR spectrometer (Purkinje General Instrument, Beijing, China). Sheet resistance was measured using the four-probe method.

Results and discussion

In a standard process, oleyamine solution containing AgBr and $CuCl_2$ was heated at 160^{o}C for 6 hours and cooled down to room temperature naturally. Grey precipitates were observed at the bottom of the flask, indicating the formation of Ag nanowires. As shown in Figure 1, A-C, the resultant products exhibited a wire-like shape (33.8±2.6 nm in width and 15±7μm in length) in high purity. It is worth pointing out that such Ag nanowires could be routinely synthesized in high purity (>98%) without involving any additional purification/separation process. To further confirm their structure and shape, we also performed a serious of measurements in addition to SEM and TEM imaging, including HRTEM, ED, EDS, and XRD. The HRTEM image (Fig. 1D) taken from an individual Ag wire shows a continuous fringe pattern with spacing of 0.236 nm, which could be indexed to the {111} reflection of face-centered cubic (fcc) Ag. Corresponding ED pattern (the inset in Fig. 1C) has more than one set of diffraction spots, suggesting its twinned structure. Figure S1 shows XRD pattern of the Ag nanowires, where the diffraction peaks occurring at 38.1^o, 44.3^o, 64.5^o, and 77.5^o are indexed as (111), (200), (220), and (311) facets, being consistent well with an fcc Ag crystalline structure (JCPDS 04-0783). No peak for other crystal types was observed. The sharp diffraction peaks indicated the sample had a high crystallinity. EDS pattern confirmed there is no other metallic element involved in the product

(Fig. S2). Taken together, we can conclude that the as-obtained Ag products had a twinned structure, together with a wire-like shape.

To understand the formation mechanism, we monitored the reaction by terminating the synthesis at different periods and taking out aliquots for SEM imaging. As shown in Figure 2A, at t=1 h, the products were dominated with nanocubes with a typical size of 168 nm. It is worth noting that these nanocubes were not stable and exhibited noticeable shape variation upon SEM electron irritation, suggesting they should be composed of AgBr instead of Ag due to their photosensitivity. To verify it, we collected those particles and performed analysis using XRD. As shown in Figure S3, their diffraction patterns could be identified to AgBr (JCPDS 79-0149) rather than Ag, which confirmed their composition. Previous studies indicated that during the synthesis of Ag nanowires, the formation of silver halides nanocubes could induce the heterogeneous nucleation of metallic Ag upon their surfaces.[46, 53] Then, Ag nanowires would subsequently grow from these nucleation sites. When the reaction continued to t=2 h, wire-like products began to appear but the yield was still low (Fig. 2B). The percentage of nanowires significantly increased as reaction proceeded to t=4 h (Fig. 2C). Even longer reaction period had little impact on the yield of wire-like products (Fig. 2D). Based on these results, the reaction pathway was schematically illustrated in Figure S4.

In the current synthesis, $CuCl_2$ was found to be necessary for Ag nanowire formation. To probe the role of Cu ions in this synthesis, a set of control experiments was conducted with the addition of different amounts of $CuCl_2$. As shown in Figure 3, A and B, if no or lower amount of $CuCl_2$ was present in the reaction solution, the purity of final products was not satisfying. Only part of the final products were nanowires and large quantities of nanoparticles could be observed. In contrast, the yield of Ag nanowires kept unchanged when the concentration of $CuCl_2$ was increased (Fig. 3, C and D). These results indicated that sufficient supply of $CuCl_2$ was necessary for the formation of wire-like products in high purity. Generally, in order to achieve high-yield formation of Ag nanowires, particles with a penta-twinned structure should survive and dominate

the seeds formed in the initial stages. In our case, Cu(I), generated in situ from the reduction of Cu(II), could effectively scavenge any adsorbed atomic oxygen from the Ag seeds, thus dampening the oxidative etching strength and protecting the penta-twinned particles from being etched.[45, 54, 55] In other word, without sufficient Cu ions, it is highly possible that those penta-twinned particles could not survive in the initial stages. As a result, Ag nanocrystals with other crystallinities may appear as final products, which made the percentage of Ag nanowires lower. In short, the concentration of $CuCl_2$ in the system could significantly influence the oxidative etching strength of Ag and thus the yield of penta-twinned Ag nanowires.

We also evaluated the effect of type of Ag precursor on product morphology. As shown in Figure 4, when the Ag precursor, AgBr, was replaced by $AgNO_3$ and AgCl, the resultant products no longer exhibited the wire-like shape. Instead, they were dominated with polyhedral particles (Fig. 4A) and porous spheres with hollow interiors (Fig. 4B), respectively. These results indicated the anions involved with the Ag precursor can cause a significant change to the morphology of final product. Compared to AgBr/Ag, the standard potential of Ag^+/Ag and AgCl/Ag are much higher (AgCl/Ag, 0.2223V; Ag^+/Ag, 0.7996 V; AgBr/Ag, 0.07133V). The reduction rate would be accelerated when AgBr was replaced by either AgCl or $AgNO_3$. As a result, the variation of Ag precursor, can significantly cause the change of reaction kinetics, which may impact the nucleation and growth pattern and thus the morphology of final products.

The current synthesis involved the use of AgBr, anhydrous $CuCl_2$, and oleyamine. At an elevated temperature, oleyamine can serve as both the solvent and the reductant to reduce Ag^+ species to zero-valent Ag.[56-59] As a result, the reaction temperature had played an important role in influencing the reaction kinetics. To evaluate the effect of reaction temperature on product morphologies, we conducted a set of control experiments. Figure 5 shows SEM images of products obtained using the standard procedure, except that the reaction temperature was changed. In particular, As reaction temperature tuned from 160 ^oC to 140, 170, 180, and 200 ^oC, the resultant products no longer exhibited the wire-like shape in high yield. In contrast, they were

dominated with a mixture of wires and particles with various shapes. As indicated in the discussion above, the synergetic effect of oxidative etching and crystal growth played an important role in the formation of Ag nanowires in high purity. When the temperature varied, the oxidative etching strength would be either enhanced or dampened. Since the amount of oxygen scavenger, $CuCl_2$ was kept unchanged, different types of seeds may survive in the initial stages and thus the percentage of those five-fold twinned seeds may become lower. In short, these results of control experiments showed that an appropriate reaction temperature was essential for the formation. Either higher or lower temperature may cause the change of oxidative etching strength, which led to the variation of crystallinities and shapes of final products.

We washed the as-prepared oleyamine-capped Ag nanowires and deposited these nanowires on PET films to test their performance as TCE (Fig. 6, A and B). As shown in Figure 6C, by varying the concentration of Ag nanowires suspensions, a series of Ag nanowires films with different thicknesses on PET films have been prepared, which modify their light transmittance from 30-40% to approaching 90%. Simultaneously, their sheet resistances increase from 3.22 to 53.5 ohm/sq, which means they have an extremely high conductive level. This conductivity level well satisfies the industrial requirements and compares with Ag nanowires networks electrodes documented in literature.

Conclusions

In summary, oleyamine-capped Ag nanowires have been successfully prepared in high purity via a simple one-pot approach. With the addition of $CuCl_2$, the reduction of AgBr by oleyamine at an elevated temperature was found to promote the formation of Ag nanowires in high yield. By monitoring the reaction, we found the AgBr nanocubes were formed in the early stage, which then served as the sites for heterogeneous nucleation and thus the formation of Ag nanowires. The amount of $CuCl_2$, type of Ag precursor, and reaction temperature were systematically evaluated to reveal their contributions to the formation of wire-like products.

Additionally, the as-prepared Ag nanowires were washed and deposited on PET films to form TCE, which exhibited good conductivity at high transparency. In addition to TCE, these products could find important applications in the fields of conductive ink, wearable electronics, among others.

Acknowledgements

This work was supported by the National Natural Science Foundation of China (No. 21175059).

Notes and references

1. Y. Xia, Y. Xiong, B. Lim and S. E. Skrabalak, *Angew. Chem. Int. Ed.*, 2009, **48**, 60-103.

2. J. Chen, B. J. Wiley and Y. Xia, *Langmuir*, 2007, **23**, 4120-4129.

3. Jingyi Chen, B. J. W. and and Y. Xia, *Langmuir*, 2007, **23**, 4120-4129.

4. C. M. Lieber, *Solid State Commun.*, 1998, **107**, 607–616.

5. J. Hu, T. W. Odom and C. M. Lieber, *Acc. Chem. Res*, 1999, **30**.

6. J. I. Pascual and J. Mendez, *Science*, 1995, **267**, 1793-1795.

7. Y. Wu, J. Xiang, C. Yang, W. Lu and C. M. Lieber, *Nature*, 2004, **430**, 61-65.

8. T. M. Whitney and J. S. Jiang, *Science*, 1993, **261**, 1316-1319.

9. B. Wu, A. Heidelberg and J. J. Boland, *Nat. Mater.*, 2005, **4**, 525-529.

10. C. J. Murphy, T. K. Sau, A. Gole and C. J. Orendorff, *MRS Bull.*, 2005, **30**, 349-355.

11. C. J. Murphy and N. R. Jana, *Adv. Mater.*, 2002, **14**, 80-82.

12. R. M. Dickson and L. A. Lyon, *J. Phys. Chem. B*, 2000, **104**, 6095-6098.

13. J. He, Y. Wang, Y. Feng, X. Qi, Z. Zeng, Q. Liu, W. S. Teo, C. L. Gan, H. Zhang and H. Chen, *ACS Nano*, 2013, **7**, 2733-2740.

14. B. Wiley, Y. Sun, B. Mayers and Y. Xia, *Chem. Eur. J.*, 2005, **11**, 454-463.

15. B. Wiley, Y. Sun and Y. Xia, *Acc. Chem. Res.*, 2007, **40**, 1067-1076.

16. X. M. Sun and Y. D. Li, *Adv. Mater.*, 2005, **17**, 2626-2630.

17. A. I. Boukai, Y. Bunimovich, J. Tahir-Kheli, J.-K. Yu, W. A. Goddard Iii and J. R. Heath, *Nature*, 2008, **451**, 168-171.

18. A. Tao, F. Kim, C. Hess, J. Goldberger, R. He, Y. Sun, Y. Xia and P. Yang, *Nano Lett.*, 2003, **3**, 1229-1233.

19. C. J. Murphy, A. M. Gole, S. E. Hunyadi and C. J. Orendorff, *Inorg. Chem.*, 2006, **45**, 7544-7554.

20. P.-C. Hsu, X. Liu, C. Liu, X. Xie, H. R. Lee, A. J. Welch, T. Zhao and Y. Cui, *Nano Lett.*, 2015, **15**, 365-371.

21. F. Xu and Y. Zhu, *Adv. Mater.*, 2012, **24**, 5117–5122.

22. S. De, T. M. Higgins, P. E. Lyons, E. M. Doherty, P. N. Nirmalraj, W. J. Blau, J. J. Boland and J. N. Coleman, *ACS Nano*, 2009, **3**, 1767-1774.

23. L. Hu, *ACS Nano*, 2010, **4**, 2955-2963.

24. S. Lee, S. Shin, S. Lee, J. Seo, J. Lee, S. Son, H. J. Cho, H. Algadi, S. Al-Sayari and D. E. Kim, *Adv. Func. Mater.*, 2015, **25**.

25. H. Lu, D. Zhang, J. Cheng, J. Liu, J. Mao and W. C. H. Choy, *Adv. Func. Mater.*, 2015.

26. T. C. Hauger, S. M. I. Al-Rafia and J. M. Buriak, *ACS Appl. Mater. Interf.*, 2013, **5**, 12663-12671.

27. L. Hu, H. Wu and Y. Cui, *MRS Bull.*, 2011, **36**, 760-765.

28. P. Kumar, M. G. Krishna and A. K. Bhattacharya, *Int. J. Nanosci.*, 2008, **7**, 255-261.

29. P. Kumar, *J. Nanopart. Res.*, 2010, **12**, 2473-2480.

30. P. Kumar, M. G. Krishna, A. K. Bhatnagar and A. K. Bhattacharya, *Int. J. Nanomanuf.*, 2008, **2**, 477-495.

31. M. G. Krishna and P. Kumar, Non-lithographic techniques for nanostructuring thin films and surfaces in Emerging nanotechnologies for manufacturing, 2009, Eds. W. Ahmed, M. J. Jackson Elsevier, ISBN 97808155, Pages 15838.

32. Z. Wang, J. Liu, X. Chen, J. Wan and Y. Qian, *Chem. Eur. J.*, 2005, **11**, 160-163.

33. B. H. Hong, S. C. Bae, C.-W. Lee, S. Jeong and K. S. Kim, *Science*, 2001, **294**, 348-351.

34. J. Q. Hu, Q. Chen, Z. X. Xie, G. B. Han, R. H. Wang, B. Ren, Y. Zhang, Z. L. Yang and Z. Q. Tian, *Adv. Func. Mater.*, 2004, **14**, 183-189.

35. N. R. Jana, L. Gearheart and C. J. Murphy, *Chem. Commun.*, 2001, **7**, 617-618.

36. P. Jiang, S.-Y. Li, S.-S. Xie, Y. Gao and L. Song, *Chem. Eur. J.*, 2004, **10**, 4817-4821.

37. S. Liu, J. Yue and A. Gedanken, *Adv. Mater.*, 2001, **13**, 656-658.

38. S. Tang, S. Vongehr, N. Wan and X. Meng, *Mater. Chem. Phys.*, 2013, **142**, 17-26.

39. W. Zhang, P. Chen, Q. Gao, Y. Zhang and Y. Tang, *Chem. Mater.*, 2008, **20**, 1699-1704.

40. Y. Sun, B. Gates, B. Mayers and Y. Xia, *Nano Lett.*, 2002, **2**, 165-168.

41. Y. Sun and Y. Xia, *Adv. Mater.*, 2002, **14**.

42. Y. Sun, Y. Yin, B. T. Mayers, T. Herricks and Y. Xia, *Chem. Mater.*, 2002, **14**, 4736-4745.

43. W. B, *Cheminform*, 2005, **11**, 454–463.

44. B. Wiley, Y. Sun and Y. Xia, *Langmuir*, 2005, **21**, 8077-8080.

45. K. E. Korte, S. E. Skrabalak and Y. Xia, *J. Mater. Chem.*, 2008, **18**, 437-441.

46. C. An, J. Wang, S. Wang, Q. Zhang, M. Yang and J. Zhan, *CrystEngComm*, 2012, **14**, 5886-5891.

47. L. R. Shobin, D. Sastikumar and S. Manivannan, *Sensor Actuat. A-Phys.*, 2014, **214**, 74-80.

48. C. Yang, H. Gu, W. Lin, M. M. Yuen, C. P. Wong, M. Xiong and B. Gao, *Adv. Mater.*, 2011, **23**, 3052-3056.

49. Y. Zheng, J. Tao, H. Liu, J. Zeng, T. Yu, Y. Ma, C. Moran, L. Wu, Y. Zhu and J. Liu, *Small*, 2011, **7**, 2307–2312.

50. B. Nikoobakht and M. A. El-Sayed, *Chem. Mater.*, 2003, **15**, 1957-1962.

51. X. Xia, J. Zeng, B. McDearmon, Y. Zheng, Q. Li and Y. Xia, *Angew. Chem. Int. Ed.*, 2011, **50**, 12542–12546.

52. L. Zhang, J. Zhang, Q. Kuang, S. Xie, Z. Jiang, Z. Xie and L. Zheng, *J. Am. Chem. Soc.*, 2011, **133**, 17114-17117.

53. W. M. Schuette and W. E. Buhro, *ACS Nano*, 2013, **7**, 3844-3853.

54. Q. Zhang, J. Xie, Y. Yu, J. Yang and J. Y. Lee, *Small*, 2010, **6**, 523-527.

55. H. Huang, Y. Wang, A. Ruditskiy, H.-C. Peng, X. Zhao, L. Zhang, J. Liu, Z. Ye and Y. Xia, *ACS Nano*, 2014, **8**, 7041-7050.

56. D. Wang, T. Xie, Q. Peng and Y. Li, *J. Am. Chem. Soc.*, 2008, **130**, 4016-4022.

57. S. Sun and A. Moser, *Science*, 2000, **287**, 1989-1992.

58. J. Zhang, H. Yang, J. Fang and S. Zou, *Nano Lett.*, 2010, **10**, 638-644.

59. S. Peng and Y. Sun, *Proc. Nat. Acad. Sci. USA*, 2010, **107**, 14530-14534.

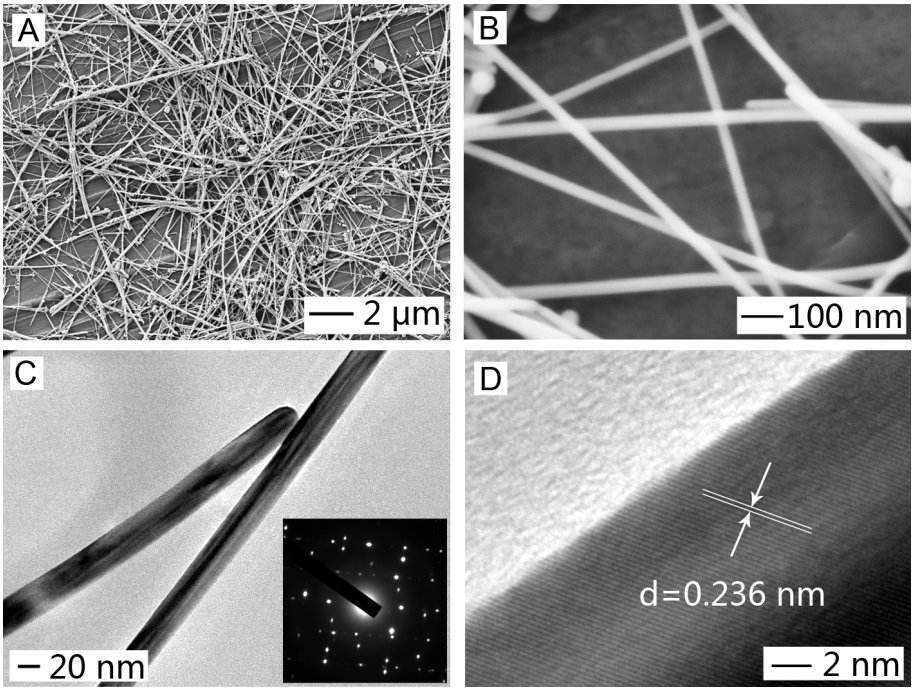

Figure 1. Characterization of Ag nanowires: (A-B) SEM images; (C) TEM and (D) HRTEM images. The inset in (C) shows electron diffraction pattern.

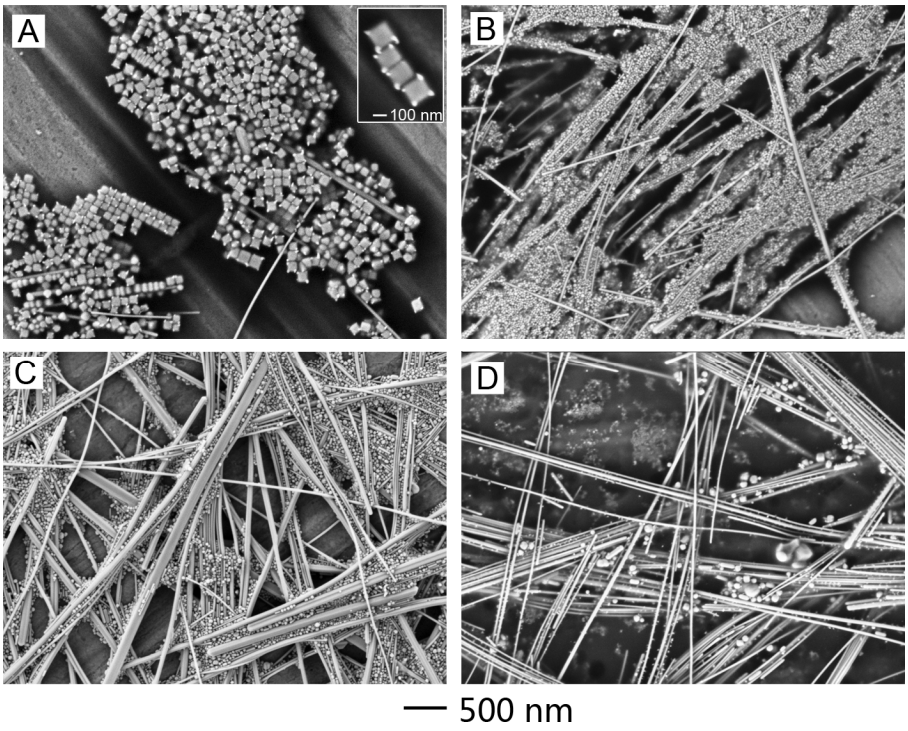

Figure 2. SEM images of an aliquot taken out from the reaction system at (A) t = 1 h; (B) t = 2 h; (C) t = 4 h; and (D) t = 12 h. The inset in (A) shows typical AgBr nanocubes.

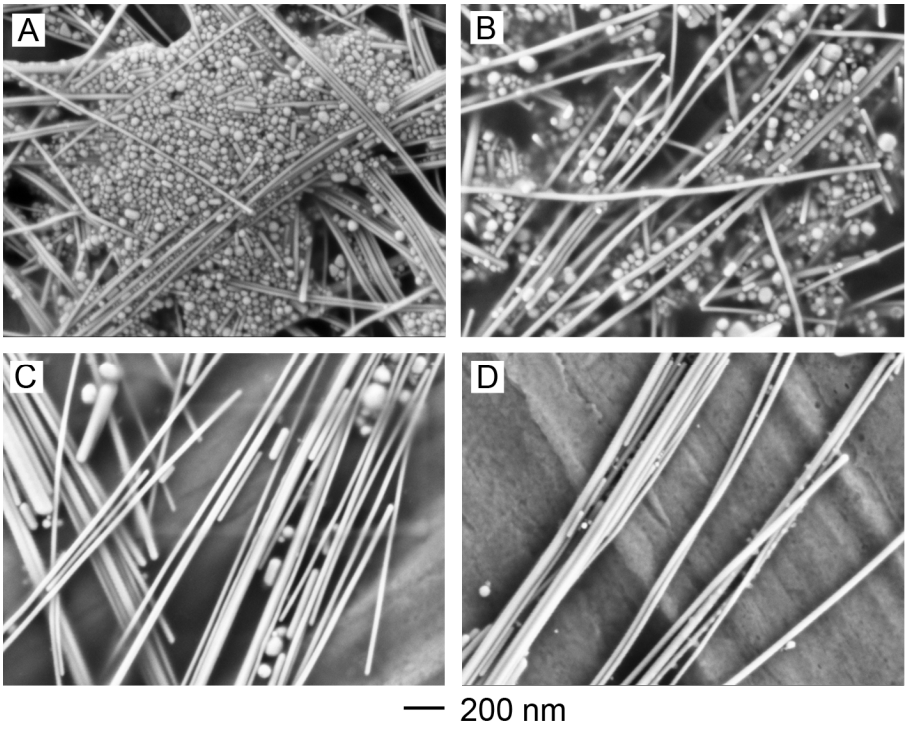

Figure 3. The effect of $CuCl_2$ amount on product morphologies. SEM images of products obtained using the standard procedure, except that the amount of $CuCl_2$ was tuned from 0.03 mg in the standard procedure to (A) 0, (B) 0.01, (C) 0.5, and (D) 2 mg, respectively. The molar ratio of $CuCl_2$ to Ag was (A) 0, (B) 1:42818, (C) 1:856.37, and (D) 1:142.73, respectively.

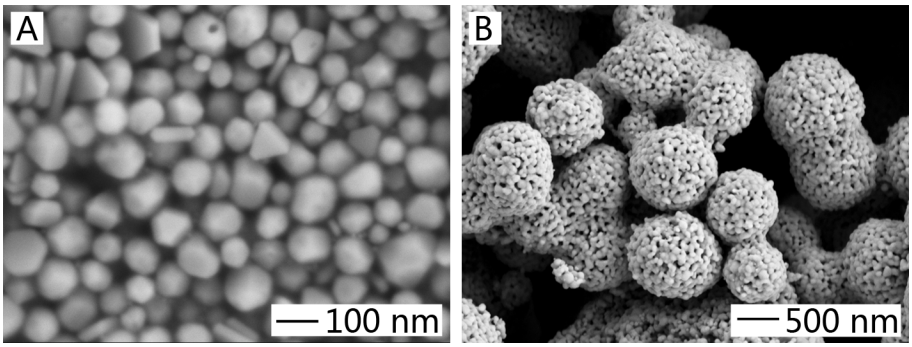

Figure 4. The effect of Ag precursor on product morphologies. SEM images of products obtained using the standard procedure, except that the AgBr was replaced by (A) $AgNO_3$ and (B) AgCl, respectively.

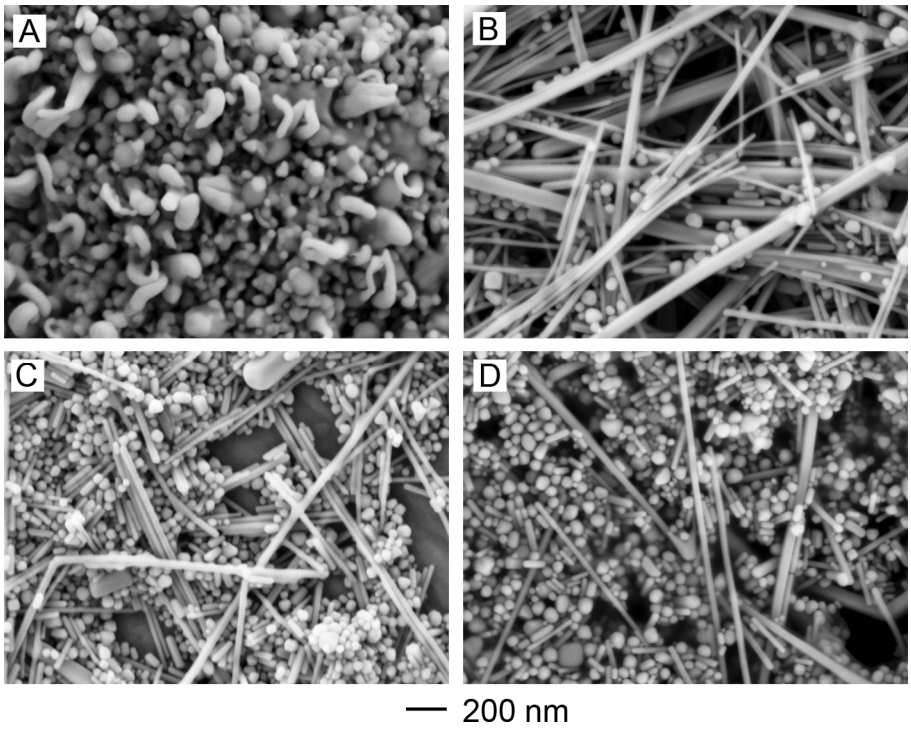

Figure 5. The effect of reaction temperature on product morphologies. SEM images of products obtained using the standard procedure, except that the reaction temperature were tuned to (A) 140, (B) 170, (C) 180, and (D) 200 ^{o}C, respectively.

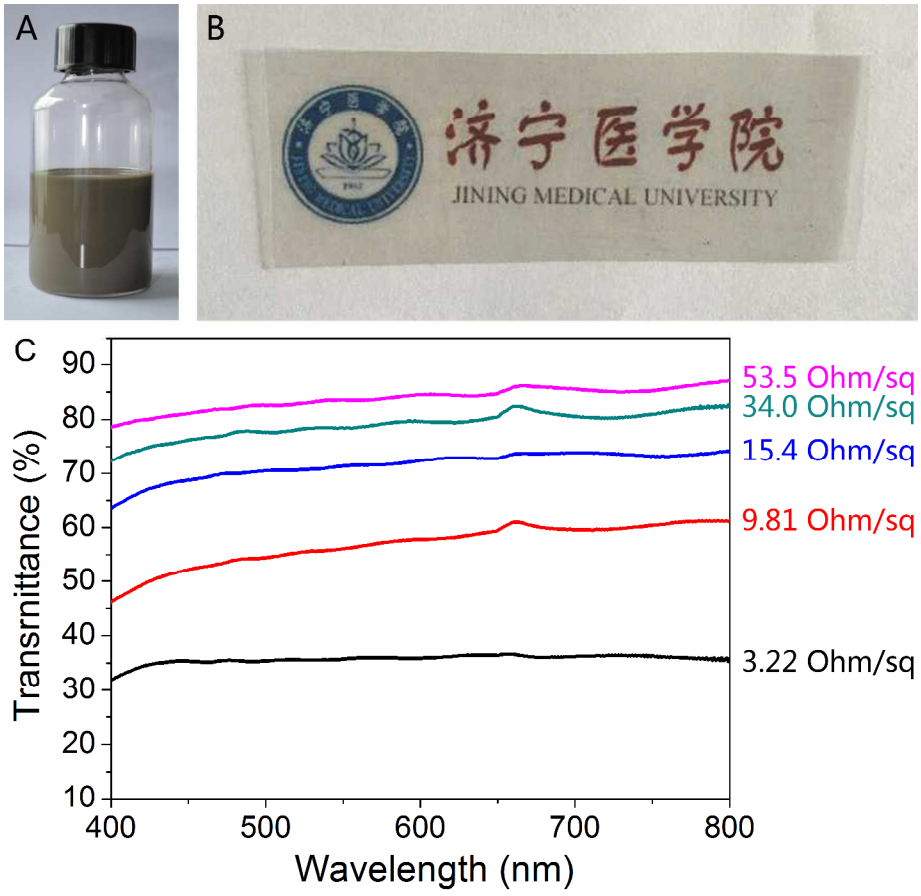

Figure 6. (A, B) Pictures of (A) a bottle of oleyamine-capped Ag nanowires suspended in hexane and (B) a piece of PET film coated with as-prepared Ag nanowires. (C) UV/vis transmission spectra of Ag nanowires films on PET with controlled transparency. The resistances decreased from 53.5 to 3.22 ohm/sq with the decrease of transparency.

Supporting Information for

Facile Synthesis of Oleyamine-Capped Silver Nanowire and Its Application for Transparent Conductive Electrode**

Jun Zhu,[a*] *Xiufang Xu,*[b] *Jinglei Liu,*[c] *Yiqun Zheng,*[b] *and Shifeng Hou*[a, c]

[a]Research Institute of Bio-nanotechnology, Jining Medical University, Jining, Shandong 272000, P. R. China

[b]Leadernano Tech L.L.C., Jining, Shandong 272000, P. R. China

[c]National Engineering and Technology Research Center for Colloidal Materials, Shandong University, Jinan, Shandong 250100, P. R. China

*Corresponding Author: Prof. J. Zhu, E-mail: jnzhuj@163.com

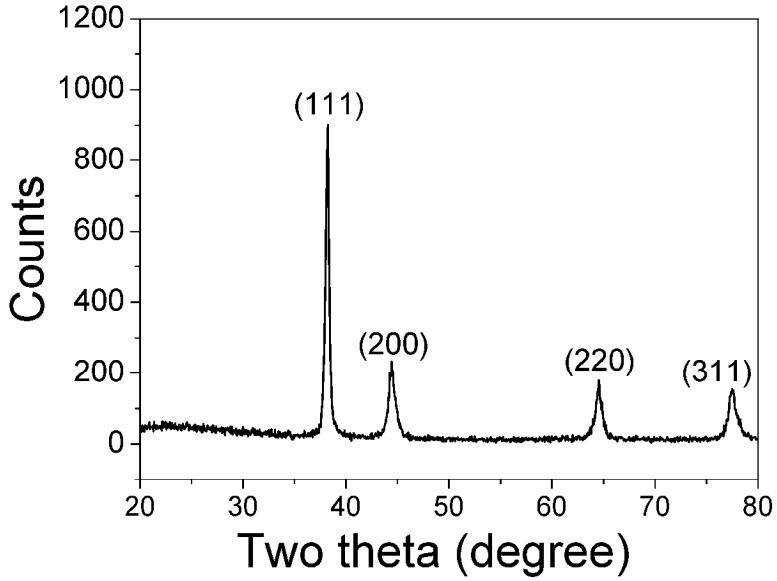

Figure S1. XRD pattern of Ag nanowires.

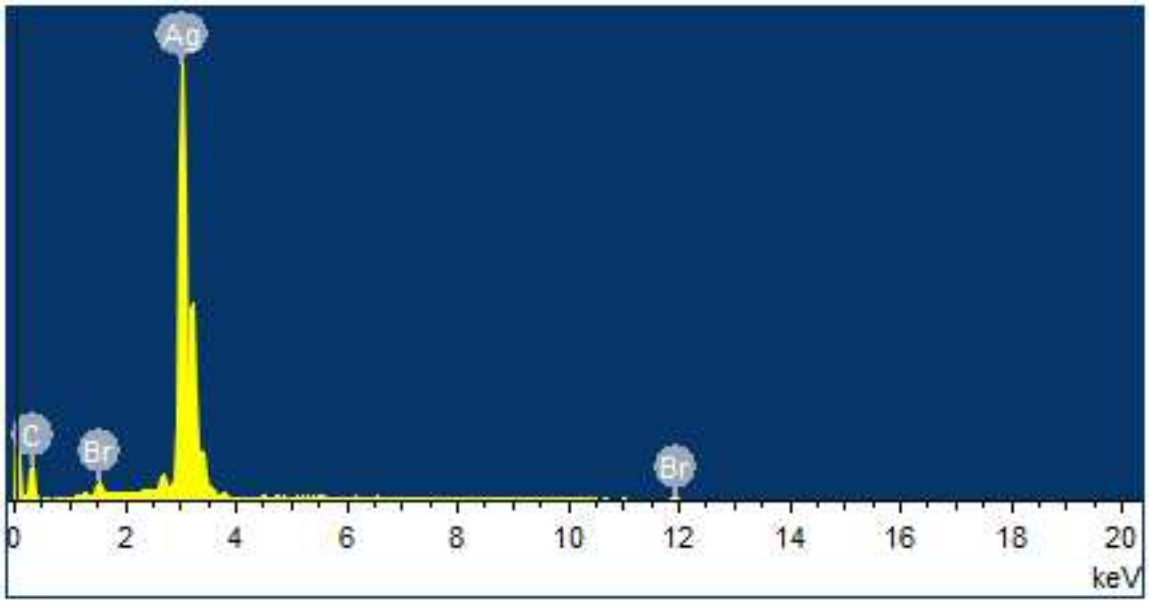

Figure S2. EDS pattern of Ag nanowires. Three elements, Ag, Br, and C, were observed in the spectrum and their mass percentage was 92.4%, 1.91%, and 5.70%, respectively. The presence of Br and C should be attributed to the residual Br^- on Ag nanowires surface and the use of conductive carbon tape during the measurement, respectively.

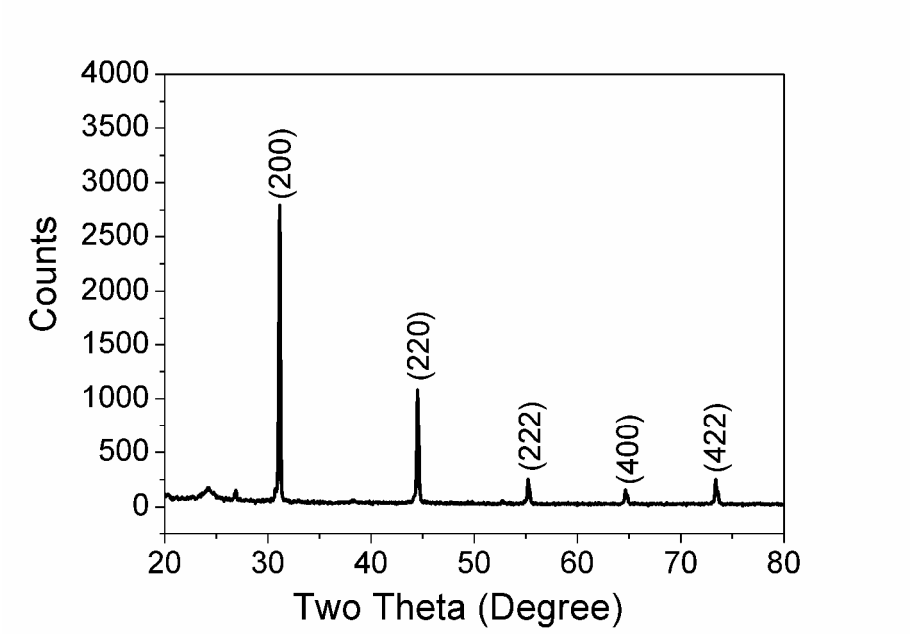

Figure S3. XRD pattern of an aliquot taken out from the reaction system at t = 1 h.

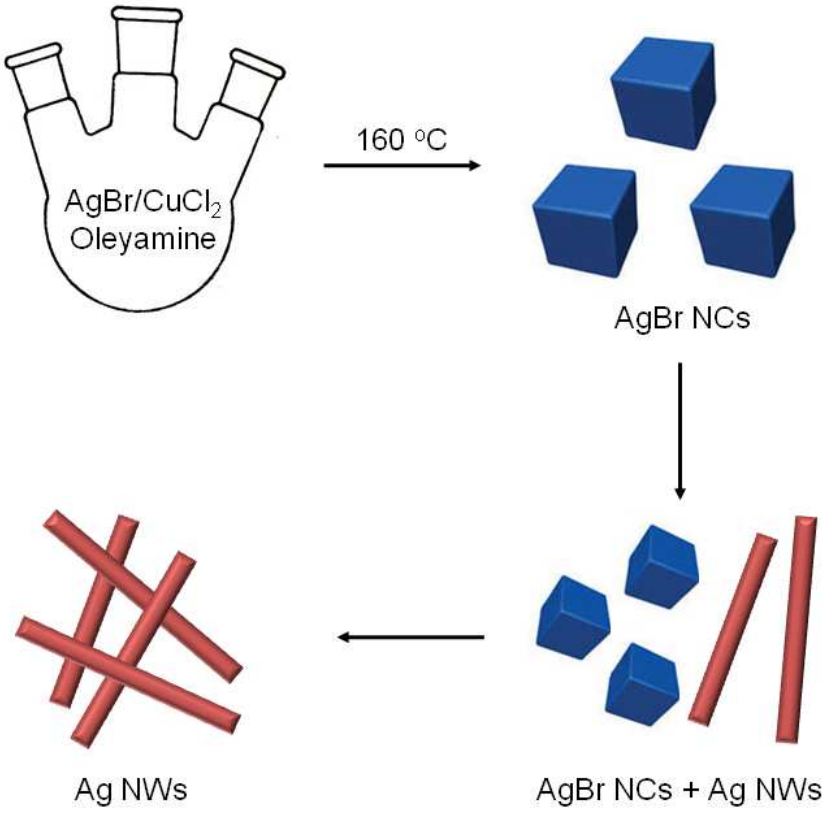

Figure S4. Schematic illustration showing the reactions and related mechanism leading to the formation of silver nanowire (NC: nanocube; NW: nanowire).

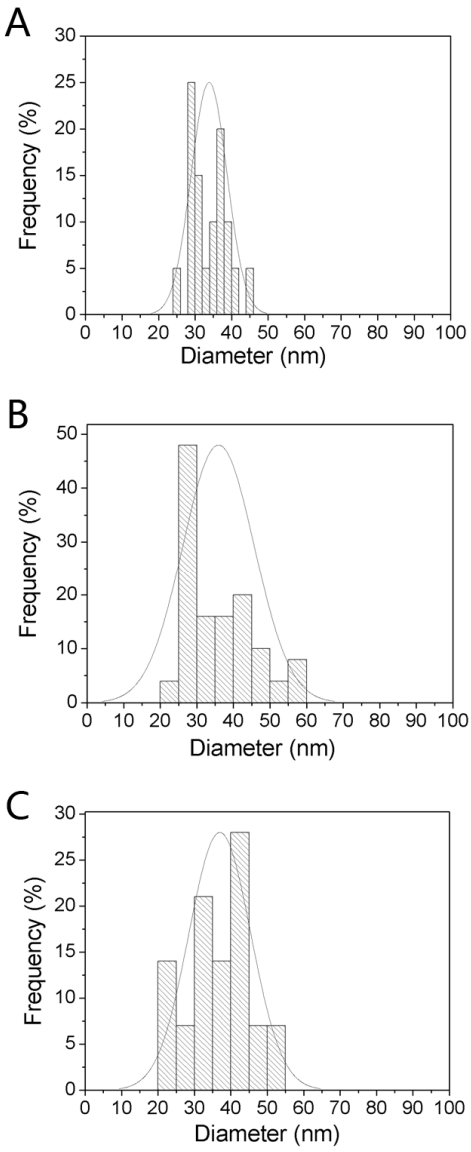

Figure S5. Histograms of nanowire diameter distribution for samples prepared under the experimental condition described in (A) Figure 1; (B) Figure 3C; (C) Figure 3D, respectively.

Table S1. Diameter of nanowires and corresponding standard deviations for samples obtained by repeating the standard procedure for three times.

	Diameter (nm)	**Standard deviation (%)**
1	33.8	7.7
2	35.1	7.3
3	34.3	7.6